NUMERICAL STUDY OF THERMAL AND STRUCTURAL STRAINS IN MULTIPASS GMAW SURFACING AND REBUILDING

GAWROŃSKA Elżbieta, WINCZEK Jerzy

Czestochowa University of Technology, Czestochowa, Poland, EU
elzbieta.gawronska@icis.pcz.pl; winczek@gmail.com

Abstract

The paper presents the calculations of temperature field, volume fractions of structural components and strains during multipass GMAW surfacing of a prismatic element made of S235 steel. The bimodal heat source model is used in the description of temperature field. The solution takes into consideration the heating caused by the welding heat source during overlaying subsequent weld beads and self-cooling of already padded areas. The highest temperatures enable to determine characteristic heat-affected zones. The critical temperatures A_1 and A_3 are used to determine partial and full austenitic transformation zones, while the temperature of solidus is used to determine the fusion line. Kinetics of phase changes during heating is limited by temperature values at the beginning (A_1) and at the end (A_3) of austenitic transformation. In order to quantitatively describe the dependence of structure and material quality on temperature and transformation time of over-cooled austenite during surfacing, time-temperature-transformation at continuous cooling (TTT) welding diagram is used. The structural and thermal expansion coefficient values are determined on the basis of authors' own dilatometric research. For calculations are used authors' programs made in Borland Delphi. The results are presented in the form of temperature and volume phase fraction distributions in the element's cross section as well as thermal cycles of volume phase fractions and strains at selected points.

Keywords: Multipass welding, temperature field, phase transformation, strains, GMA

1. INTRODUCTION

Modeling of thermo-mechanical states of surfacing process involves the proper determination of the temperature field, the quantitative perspective on phase transformations, and the determination of deformations, which is the basis for determining strains. Based on the analytical descriptions given in [1] by the authors of this study, there were performed analysis of welding thermal cycles, volume fractions of phases, thermal and structural strains in multipass GMAW surafacing of the welded plate with dimensions of 0.4 x 0.4 m and thickness of 0.03 m made of S235 steel. Numerical simulations were performed for the example of making five welds of 0.2 m length in the middle of the plate (coordinate o the weld beginning x_0 = 0.1 m). The following welding parameters were assumed U = 24.3 V, I = 232 A, welding speed v = 0.007 m / s, the electrode wire diameter d = 1.2 mm, electrode wire feed speed v_e = 0.013 m / s, and the size of the weld h_w = 2.77 mm, and w_w = 11.93 mm. The welding overlap was obtained assuming the distance between the axes of the individual weld beads equal 8 mm. Thermal properties of the surfaced material and the electrodes are defined by $a = 8 \cdot 10^{-6}$ m^2 / s, c = 670 J / (kg K), density of sample and electrode material $\rho = \rho_e$ = 7800 kg / m^3 i latent heat L = 268 kJ / kg. Borland Delphi development environment was used in calculations.

2. TEMPERATURE FIELD AND WELDING THERMAL CYCLE

In the calculations of the temperature field the heat source with power of 3552 W was assumed, which corresponds to the welding power with a coefficient of efficiency η = 0.63. A source associated with the operation of the electric arc with the Gaussian distribution of power density is characterized by z_0 = 0.0062 m and t_0 = 0.001 s. The maximum values of the temperature field in the cross section (**Fig. 1**) allowed for the determination of characteristic heat-affected zones (**Fig. 2**). Solidus temperature of 1493 °C determines the

weld line, and the temperatures A_1 = 720 °C and A_3 = 835 °C determine austenitic transformation zones: partial (between A_1 and A_3) and total (above A_3).

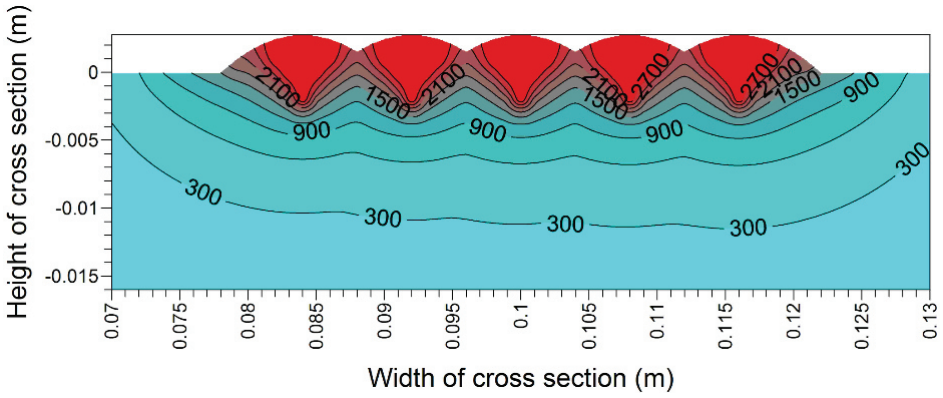

Fig. 1 The field of the maximum temperature in middle part of cross section.

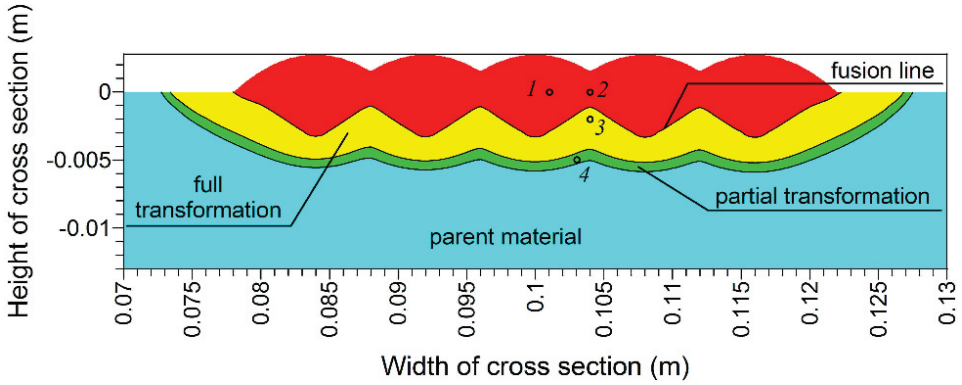

Fig. 2 Heat affected zones

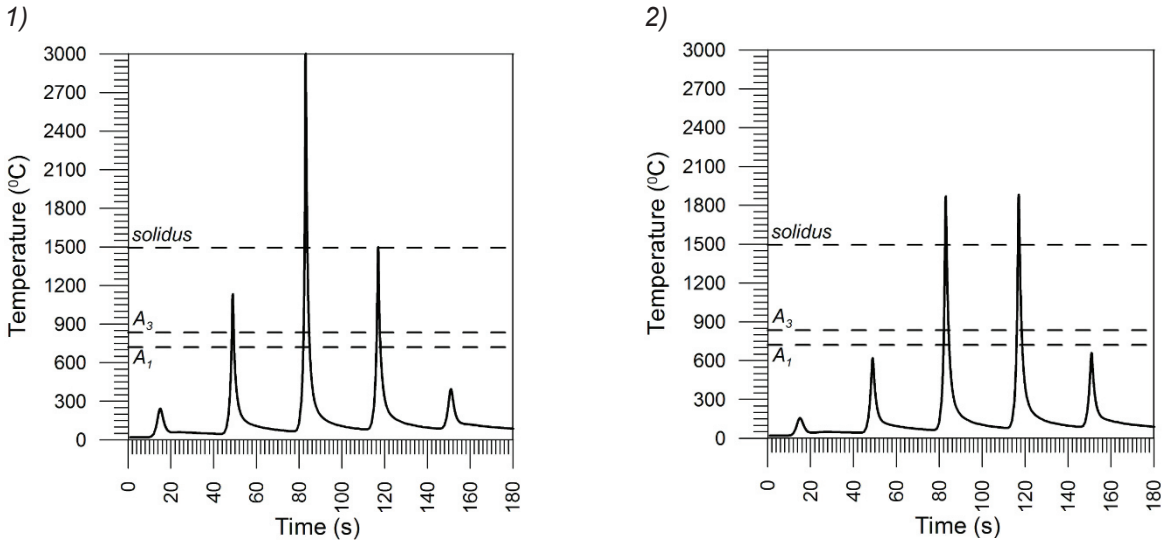

Fig. 3 Thermal welding cycles at points *1* and *2*

3) 4)

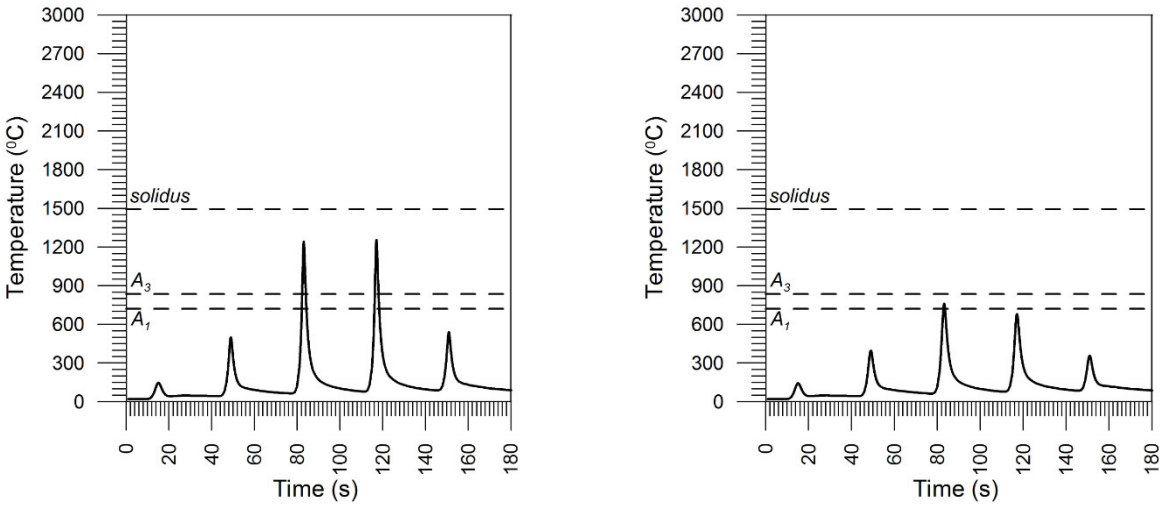

Fig. 4 Thermal welding cycles at points *3* and *4*

In the figure, the selected cross section points were marked, for which an analysis of the welding thermal cycles, phase transformations and dilatometric graphs were performed. **Fig. 3** and **4** present heat cycles in points 1-4. In all of the drawings peaks illustrate maximum temperatures during subsequent weld beads. In point 1 the temperature of the plate material exceeds the austenitizing temperature during the second weld bead, and then the material is melted twice during application of the third and fourth weld. In point 2 at the border of the third and fourth weld the temperature while applying these welds exceeds twice the melting point. In point 3, the material is not melted, but when making weld bead 3 and 4 it exceeds the temperature of full austenitizing. In point 4, the temperature exceeds the temperature A_1 but does not exceed the temperature A_3, which leads to incomplete austenite conversion during the third weld bead.

3. SIMULATION OF CHANGES OF PHASE TRANSFORMATION SHARES

The phase transformations kinetics during heating is limited by the temperatures A_1 of the beginning and A_3 the end of the austenite transformation, while the progress of phase transformations during cooling was determined on the basis of TTT-welding diagram for S235 steel shown in **Fig. 5** [2]. The applied computational model allows to determine the shares of particular phases at any point of the element for any chosen time. After completion of the surfacing process (the material cools) the calculated percentage of bainite in the weld area ranges from 63 % to 100 %. The largest share of bainite was determined in areas where single austenitization occured. In the zones where the secondary austenitization occurred when making subsequent weld beads share of bainite amounts to from 60 % to 70%. The share of perlite in complete transformation zone and fusion zone is 12 % and grows to the value of 30 % in incomplete transformation zone in the area of parent material. The changes in phase shares at selected points of the cross section (comp. **Fig. 2**) are presented in **Fig. 6** and **7**.

4. COMPUTATIONS OF THERMAL AND STRUCTURAL STRAINS

The structural strains resulting from different densities of individual structures are related to phase transformations, which in conjunction with the thermal strains leads to complicated history of strains during repeated thermal cycles. In strain calculations there was assumed a linear expansion coefficient of particular structural elements and structural strains (**Table 1**) determined on the basis of the author's own dilatometric research [3]. Dilatometric graphs for the selected cross-sectional points were shown in **Fig. 8** and **9**. In these graphs applied numbers refer the successive thermal cycles associated with application of particular welds.

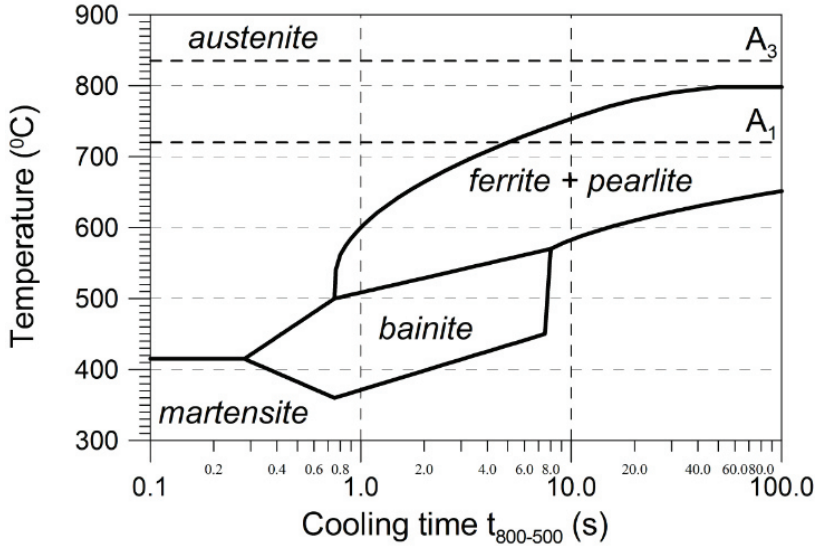

Fig. 5 TTT-welding diagram for S235 steel

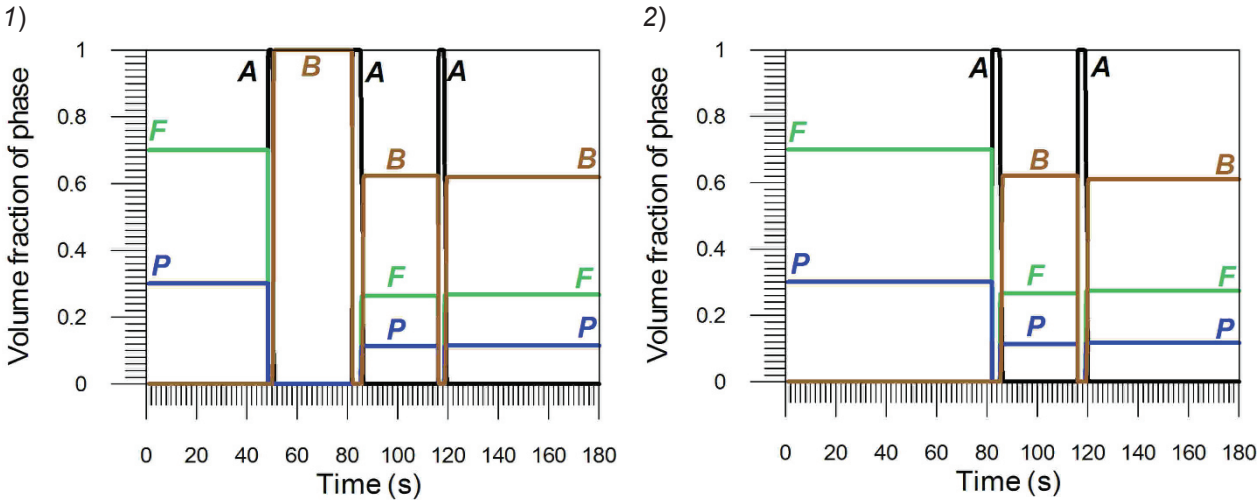

Fig. 6 Volume fraction changes at points *1* and *2* of cross section

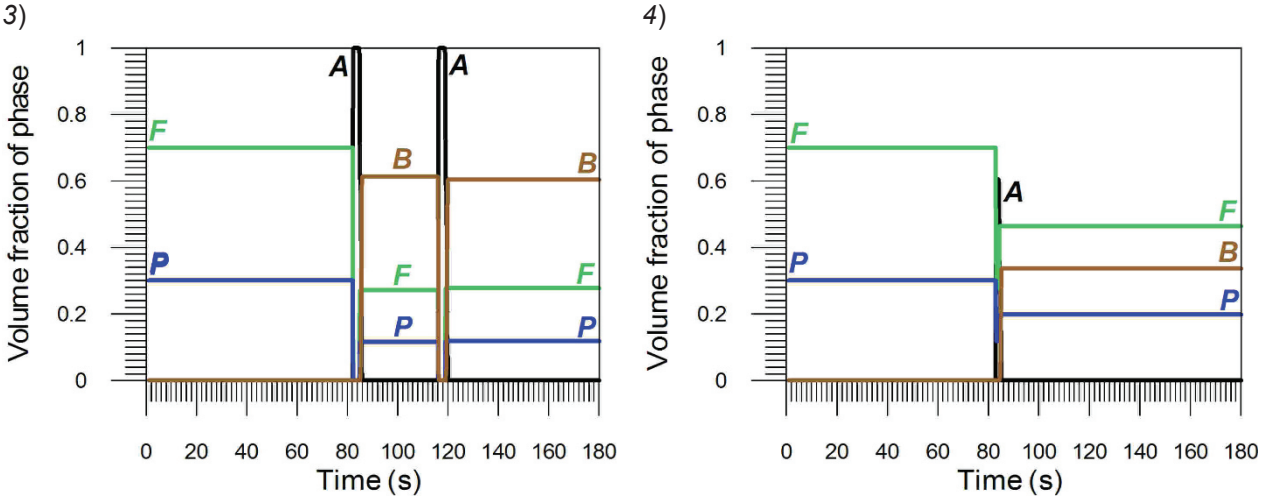

Fig. 7 Volume fraction changes at points *3* and *4* of cross section

Table 1 Structural (γ) and thermal (α) expansion coefficients of phases

	α [1/°C]		γ
Austenite	$2.178 \cdot 10^{-5}$	$\gamma_{F,P,S \rightarrow A}$	$1.986 \cdot 10^{-3}$
Ferrite	$1.534 \cdot 10^{-5}$	$\gamma_{B \rightarrow A}$	$1.440 \cdot 10^{-3}$
Pearlite	$1.534 \cdot 10^{-5}$	$\gamma_{A \rightarrow F,P}$	$3.055 \cdot 10^{-3}$
Bainite	$1.171 \cdot 10^{-5}$	$\gamma_{A \rightarrow B}$	$4.0 \cdot 10^{-3}$
Martensite	$1.36 \cdot 10^{-5}$		

In point *1*, the maximum temperature of the first cycle does not exceed the temperature of the beginning of austenitizing, there was no phase transformations and the graph is rectlinear. In the second cycle, a complete austenitic transformation occurred during heating, and then (in the temperature range 499 °C - 360 °C) the transformation of austenite to bainite, which is illustrated by a fault in the graph marked with a black line and digit *2*. In the third cycle, while heating the complete austenitic transformation occurs (*3*), and then melting (graph fault indicated by a dotted line). After solidification of the material a graph begins at 1493 °C (blue line - digit *3*) with a rectilinear section (to a temperature of 589 °C) reflecting the shrinkage of the material. Cooling transformations are causing faults in the graph to a temperature of 368 °C, then a graph again assumes the shape of a straight line. In the fourth cycle a complete transformation and the melting of the material occurs again during heating (red line). After solidification a graph (blue line) coincides with the line of deformations from the previous cycle until the start of cooling phase transformations, where the lines are slightly shifted relatively to each. In the fifth cycle phase transformations do not occur, and a graph is rectilinear.

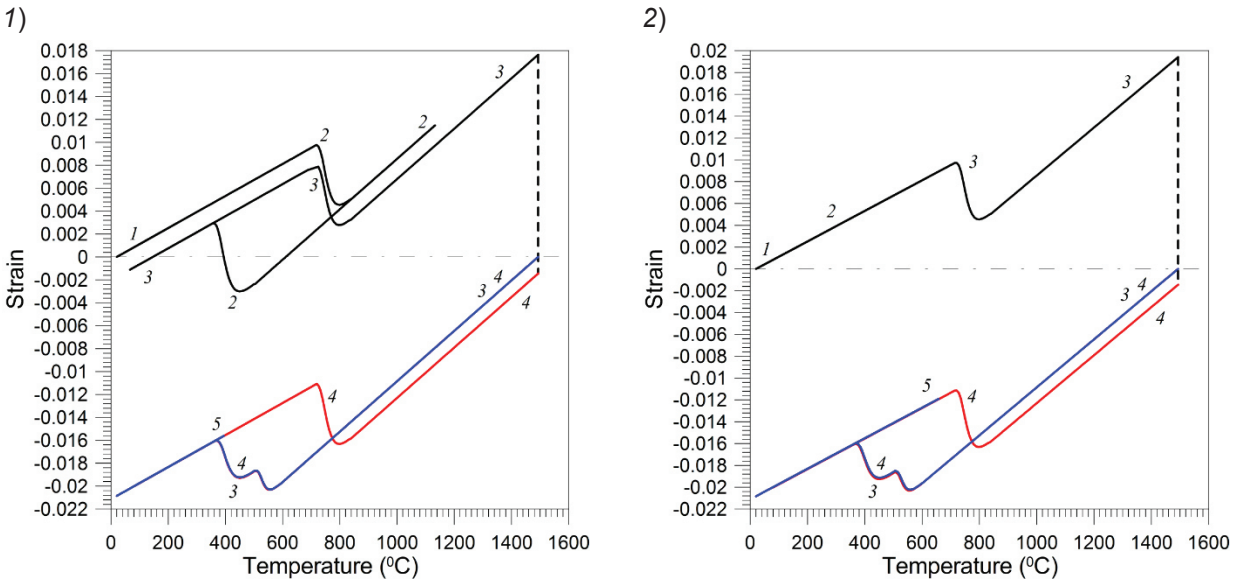

Fig. 8 Dilatometric diagrams for points *1* and *2* of cross section

In point *2* (at the border of the third and fourth weld) during the first two cycles, the temperature does not exceed the temperature at the beginning of austenitization (black line). In the third cycle, the complete austenitic transformation occurs during heating (black line - digit *3*) and then remelting is observed (dashed line). After solidification (blue line - digit *3*) a straight section of the graph ends at 590 °C with faults reflecting cooling transformations that take place. In the fourth cycle during heating again the complete austenitization (red line) and remelting (dashed line) occur, and then the solidified material shrinkage (blue line - digit *4*) to a temperature of 595 °C, when the cooling phase transformations began. In the fifth cycle, there were no phase transformations and the graph has rectilinear shape.

In point *3* of a complete transformation zone (the material has not been melted during the entire surfacing process) a dilatometric graph retains its continuity. In the first two cycles, the temperature does not exceed the initial temperature of austenitization and the graph remains rectilinear. In the third cycle, complete austenitization occurred during heating, whereas during cooling the austenite was converted into the hardening structures, which is visible in the form of characteristic faults on the graph. Similar phenomena occurred in the fourth cycle, the graphs for the third and fourth cycle are clearly shifted. In the fifth cycle, there were no phase transformations and graph retains rectilinear character. In point *4* the incomplete conversion of austenitic occurred in the third cycle

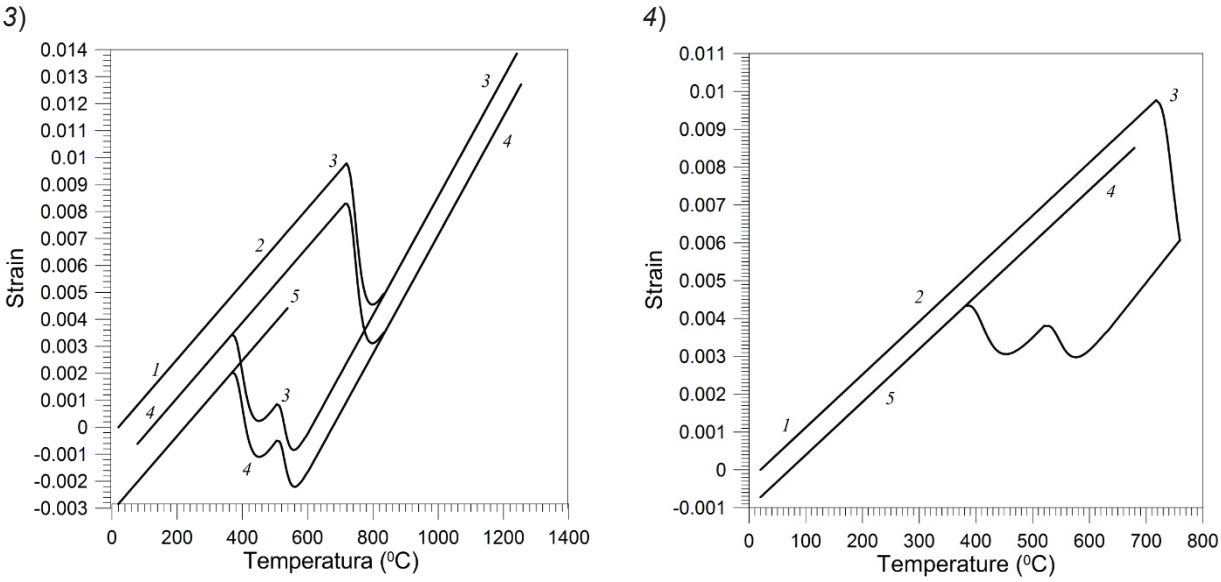

Fig. 9 Dilatometric diagrams for points *3* and *4* of cross section

5. CONCLUSION

The paper presents the results of calculations of thermal and structural strains during welding process using GMAW multipass method. Following the determination of the variable temperature fields, the heating phase transformations were considered with reference to the temperatures of the beginning and end of austenite transformation, subjecting them to the chemical composition of steel, whereas the cooling phase transformations were calculated on the basis of TTT- welding diagram. Calculated welding heat cycles and volume shares of particular structural components allowed for the determination of the size of the thermal and structural strains. In case of multi-pass surfacing or rebuilding by welding, complex thermal cycles cause multiple phase transformations resulting in significant changes in the strains in the heat affected zone, which requires consideration in the welding process modeling. The obtained results provide the basis for calculating the strain states.

REFERENCES

[1] WINCZEK J., GAWROŃSKA E. Analytical description of thermal and structural strains in multipass GMAW surfacing and rebuilding, 24-th International Conference on Metallurgy and Materials, Brno 2015 (in print)

[2] BRÓZDA J., PILARCZYK J, ZEMAN M, TTT-welding diagrams transformation of austenite, Śląsk, Katowice 1983

[3] WINCZEK J., KULAWIK A. Dilatometric and hardness analysis of C45 steel tempering with different heating-up rates, Metalurgija, Vol. 51, No 1, 2012, pp. 9 - 12